

Quadratic soliton self-reflection at a quadratically nonlinear interface

Ladislav Jankovic, Hongki Kim,* and George Stegeman

School of Optics/Center for Research and Education in Optics and Lasers, University of Central Florida, 4000 Central Florida Boulevard, Center for Research and Education in Optics and Lasers Building, Orlando, Florida 32816-2700

Silvia Carrasco and Lluís Torner

Institut de Ciències Fotòniques and Department of Signal Theory and Communications, Universitat Politècnica de Catalunya, 08034 Barcelona, Spain

Mordechai Katz

Electro-Optics Division, Soreq Nuclear Research Center, Yavene 81800, Israel

Received May 22, 2003

The reflection of bulk quadratic solutions incident onto a quadratically nonlinear interface in periodically poled potassium titanyl phosphate was observed. The interface consisted of the boundary between two quasi-phase-matched regions displaced from each other by a half-period. At high intensities and small angles of incidence the soliton is reflected. © 2003 Optical Society of America

OCIS codes: 190.4410, 190.5530.

The reflection and transmission of optical waves incident onto a boundary is governed by the well-known Snell law and Fresnel equations. For optically nonlinear media, intensity-induced changes in their optical properties occur, and the classic Snell and Fresnel equations are no longer valid.¹ If a light beam is incident at near grazing incidence from a medium with higher index (n_h) onto the boundary with a lower-index (n_l) medium characterized by a large intensity-dependent Kerr-type refractive index $n_2 > 0$ ($\Delta n = n_2 I$, where I is the intensity), it can be totally reflected at low intensities but transmitted at high intensities.² The incident radiation increases refractive index n_l locally near the boundary to values higher than n_h , permitting transmission through the boundary. This yields a variety of new phenomena, which include the power-dependent reflection of solitons at the interface between cubic nonlinear media.³

Quadratic nonlinearities also cause self-effects through nonlinear phase shifts, and similar phenomena at the interface between two quadratic materials with different nonlinear properties have been predicted.^{4–7} In particular, changes in quadratic nonlinearity at an interface can also change reflection–transmission properties, even when the refractive index is continuous across the boundary. Specifically, a planar interface in a ferroelectric medium separating two periodically poled regions with poling patterns shifted by, e.g., a quarter of a period (Λ) relative to each other was analyzed.⁷ It was found numerically that an incident quadratic spatial soliton creates an intensity-dependent potential well at the interface for the soliton. Whether the soliton is reflected from or transmitted through this interface depends on the magnitude of the potential well (intensity) and the distance over which the soliton interacts with the boundary (angle of incidence). At low intensities and (or) large incident angles, the soliton passes

through the boundary, whereas at high intensities and at small incidence angles the soliton is reflected.⁷ This beam reflection is a genuine soliton feature, as only nonlinear waves are affected by the induced potential well and it is their particlelike nature that allows solitons to retain their entity after reflection. In this Letter we experimentally verify the existence of this intensity-dependent nonlinear reflection for a half-grating period dislocation in a periodically poled potassium titanyl phosphate (PPKTP) sample.

Figure 1, which displays the outcome of typical numerical simulations of the evolution of light under experimental conditions, illustrates the concept. Figure 1(a) shows the low-power soliton transmission through the interface, and Fig. 1(b) shows the self-reflection of a higher-power input. Ideally, the soliton reflection is produced by an abrupt wave-vector-mismatch edge dislocation induced by the periodic poling longitudinal shift. In practice, such a shifted period can produce an intermediate region of finite thickness, for which the nonlinearity might be drastically suppressed (see Fig. 2). On physical grounds, the effects should still occur for thin (fraction of the soliton width) intermediate regions. The question is whether thick dislocations can spoil the effect. Our numerical simulations predict that nonlinear soliton reflection should occur even with thick linear regions separating the periodically poled regions, indicating the remarkable robustness of the effect. Figure 1(c) shows a typical example of the numerical calculations for our specific experimental sample conditions. These predictions were fully confirmed by our experimental observations, described below.

The sample was a 7.5-mm-long periodically poled PPKTP crystal.^{8,9} Spatial solitons were studied extensively in this material previously, and their properties are well understood.^{10,11} PPKTP is an attractive medium because its large measured angular

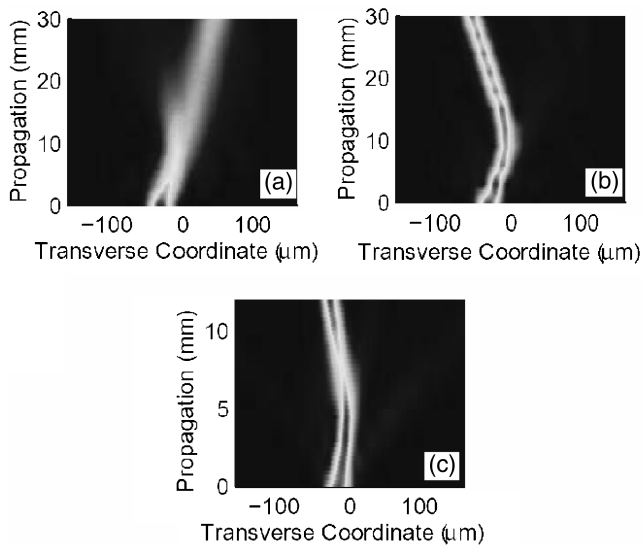


Fig. 1. Illustrative cw simulations. Top views of the evolution of a $16.5\text{-}\mu\text{m}$ waist fundamental beam incident at an input internal angle of 0.25° onto the interface in a PPKTP sample for a small positive wave-vector mismatch: (a) intensity, 3 GW/cm^2 ; initial separation from the interface, two beam widths; (b) intensity 7 GW/cm^2 ; initial separation from the interface, two beam widths; (c) intensity, 7 GW/cm^2 ; initial separation from the interface, one beam width. Thickness of the intermediate region, 0.4 beam width. All simulations were conducted with the actual quasi-phase-matched (QPM) structure (i.e., fast-varying periodical poling) rather than with averaged models.

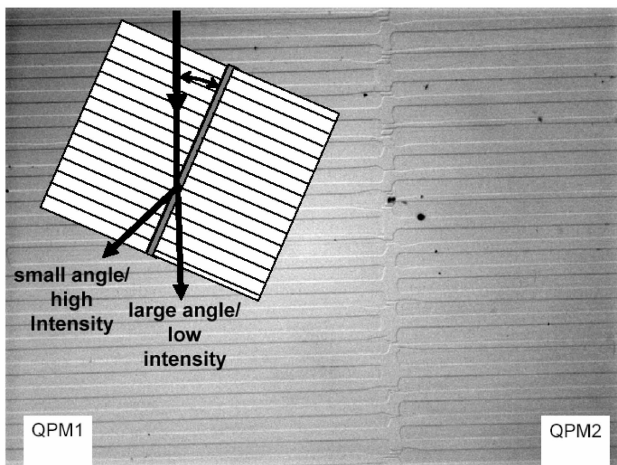


Fig. 2. Microscope picture of the sample QPM gratings and the boundary. Inset, geometry of the light beam-sample interaction.

bandwidth for soliton generation means that the solitons are essentially unchanged for small changes in incident angle. Furthermore, PPKTP's high effective nonlinearity of 9.5 pm/V (for a 50% poling duty cycle) permits soliton generation at intensities for which multiphoton absorption can be ignored. Finally, the material can be investigated at room temperature with intensities in the range of tens of gigawatts per square centimeter without photorefractive damage. A relatively low coercive field of $3.8\text{--}4.0\text{ kV/mm}$ was

used during the low-temperature poling to minimize the natural tendency of the poled lines to expand along the b axis, allowing two very close (separation of a few micrometers) grating structures to be fabricated without merging.^{8,9} A nominal $9\text{-}\mu\text{m}$ poling period along the crystal's a axis gave noncritical phase matching at 1064 nm at a temperature of $\sim 36^\circ\text{C}$ for propagation along the a axis.⁸⁻¹⁰ The mask used for the poling had a half-period phase shift, and the interface in the $a\text{-}c$ plane was located approximately in the middle of the sample. The interface region extends laterally over approximately $3\text{--}6\text{ }\mu\text{m}$ along the b axis, as indicated in the microscope picture in Fig. 2.

An EKSPLA 10-Hz Nd:YAG laser operating at 1064 nm was used for all the experiments described here. We used 25-ps (bandwidth, 0.14 nm) pulses, and, after spatial filtering, the output beam had a beam quality factor of $M^2 \approx 1.0$. The input beam waist ($1/e^2$ of intensity) at focus was $\sim 16.5\text{ }\mu\text{m}$, corresponding to five diffraction lengths in PPKTP. The energies and spatial distributions of both input and output pulses were monitored on a shot-to-shot basis by energy detectors and cameras. The shot-to-shot variation in the pulse energies was $\pm 2\%$ rms.

The solitons were launched at 28°C at angles of $\approx 0.5^\circ$ relative to the a axis. For this 2.4π phase mismatch, multiple-soliton generation is not expected, and the single-soliton threshold is approximately 4 GW/cm^2 .^{12,13} The maximum input fundamental peak intensity used was $6\text{--}7\text{ GW/cm}^2$.

We obtained the outputs shown in Fig. 3 by translating the sample from left to right (i.e., from region 2 to region 1) relative to the fixed input beam at a constant external angle of 0.5° relative to the a axis with input intensities of $\approx 6\text{ GW/cm}^2$. The experimentally observed occurrence of the reflected soliton is dependent on the angle of incidence. The main features of the soliton reflection remain the same with the increase in angle, but the input beam's intensity threshold for achievement of reflection increases with angle. However, details and magnitudes of the changes are still under experimental investigation. We focus on the second-harmonic beam, which is the beam that is most affected by the interface. In the extremes, Figs. 3(a) and 3(d), the beam propagates in each of the poled regions separately. The sample quality is clearly excellent, as evidenced by the classic soliton beams observed. In Fig. 3(b) the incident beam hits the interface near the sample's input facet, and the light is partly guided by this interface but is mostly transmitted through the interface into region 2. The reflected beam is low intensity, exhibits an irregular shape, and is not a soliton. In Fig. 3(c) the incident beam excites a soliton, which hits the interface near the sample's middle and is reflected back into region 1 as a soliton.

The dependence of the soliton's reflection on incident intensity is shown in Fig. 4. Here the interaction occurs approximately halfway through the sample. The critical intensity for reflection depends on numerous parameters, including the input beam's angle and the sample temperature-wave-vector mismatch. For

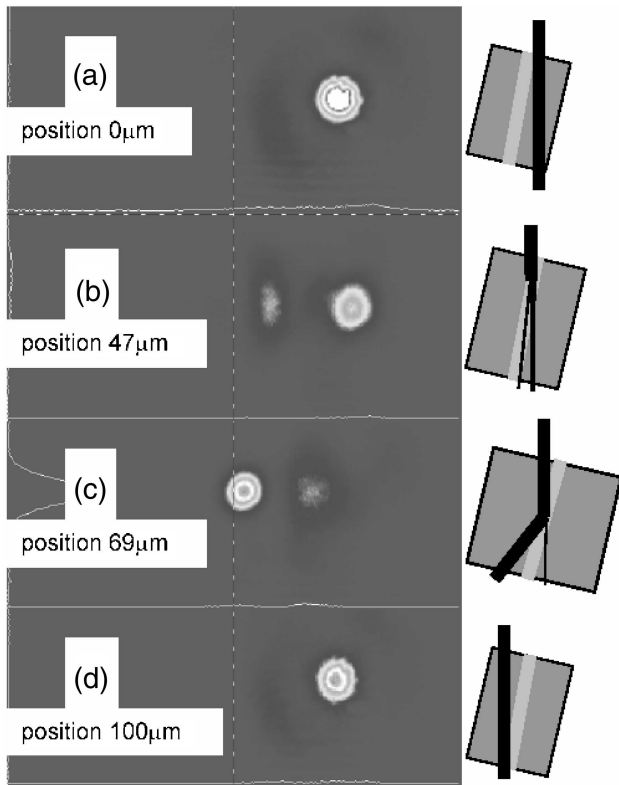


Fig. 3. Collage of beam geometries (right-hand side) and output beam distributions for several relative sample input beam positions. (Second-harmonic generation output spatial distribution is shown.) Input intensity, 6 GW/cm^2 ; incidence angle, approximately 0.5° . The transverse beam positions given are relative to (a) (at $0 \mu\text{m}$).

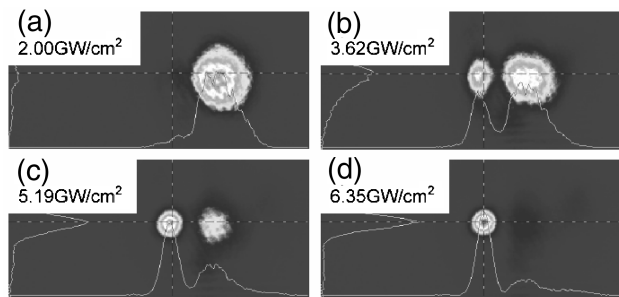


Fig. 4. Output beam distributions for beam incidence on the boundary in the middle of the sample for increasing input intensities. (Second-harmonic generation distribution at the end of the sample is shown.)

Fig. 4 this critical threshold intensity is approximately $5\text{--}6 \text{ GW/cm}^2$. At intensities below the soliton generation threshold of 4 GW/cm^2 , the beam is fully transmitted to region 2, where it diffracts. For increasing input intensity above the soliton generation threshold [Figs. 4(b) and 4(c)], the beam is partially transmitted and partially reflected, as expected from the numerical calculations [Fig. 1(a)]. With further increase in input intensity, the reflected beam takes progressively more of the input intensity, and the transmitted beam again diffracts and diminishes in intensity. Well-defined solitons carry almost all the input power on reflection from the interface in Fig. 4(d).

There are two possible reasons for the existence of partially transmitted beams. First, the experiments were conducted with pulses, which have an intensity distribution. The high-intensity parts can be preferentially reflected by the interface, whereas the wings may be transmitted. For increasingly high intensities, a progressively larger fraction of the input pulse will be reflected as solitons, as observed experimentally. Second, simulations (not included here) have shown that this beam splitting at the QPM interface can also be caused by inelastic scattering, which increases when the interface's sharpness and thickness depart from ideal.

In summary, we have observed, for the first time to our knowledge, nonlinear reflection of quadratic solitons from a purely nonlinear dislocation interface in a quasi-phase-matched structure in periodically poled KTP. The reflection coefficient was found to depend on the input intensity, as predicted by theory. This observation makes possible several soliton processing schemes, including the power-controlled steering and trapping of soliton beams with different potential wells created with engineered QPM gratings.

The authors thank Eric Johnson for taking and preparing the microscope sample pictures. This research was supported by a U.S. Army Research Office Multidisciplinary University Research Initiative and the National Science Foundation in the United States and by the Generalitat de Catalunya by the Spanish government through grant TIC2000-1010. L. Jankovic's e-mail address is ljankovi@mail.ucf.edu.

*Present address, Department of Physics, Dong-Eui University, Busan 614-714, Korea.

References

1. E. Kaplan, *JETP Lett.* **24**, 114 (1977) [*Pis'ma Zh. Eksp. Teor. Fiz.* **24**, 132 (1976)].
2. P. W. Smith and W. J. Tomlinson, *IEEE J. Quantum Electron.* **QE-20**, 30 (1984).
3. A. B. Aceves, J. V. Moloney, and A. C. Newell, *Phys. Rev. A* **39**, 1809 (1989).
4. G. I. Stegeman, D. J. Hagan, and L. Torner, *Opt. Quantum Electron.* **28**, 1691 (1996).
5. A. D. Capobianco, C. De Angelis, A. Laureti Palma, and G. F. Nalesso, *J. Opt. Soc. Am. B* **14**, 1956 (1997).
6. C. B. Clausen and L. Torner, *Phys. Rev. Lett.* **81**, 790 (1998).
7. C. B. Clausen and L. Torner, *Opt. Lett.* **24**, 7 (1999).
8. A. Englander, R. Lavi, M. Katz, M. Oron, D. Eger, E. Lebiush, G. Rosenman, and A. Skliar, *Opt. Lett.* **22**, 1598 (1997).
9. G. Rosenman, A. Skliar, D. Eger, M. Oron, and M. Katz, *Appl. Phys. Lett.* **73**, 3650 (1998).
10. H. Kim, L. Jankovic, G. I. Stegeman, M. Katz, S. Carrasco, and L. Torner, *Appl. Phys. Lett.* **81**, 2710 (2002).
11. H. Kim, L. Jankovic, G. Stegeman, S. Carrasco, L. Torner, D. Eger, and M. Katz, *Opt. Lett.* **28**, 640 (2003).
12. S. Carrasco, S. Polyakov, H. Kim, L. Jankovic, G. I. Stegeman, J. P. Torres, L. Torner, and M. Katz, *Phys. Rev. E* **67**, 46616 (2003).
13. S. Polyakov, L. Jankovic, H. Kim, G. Stegeman, S. Carrasco, L. Torner, and M. Katz, *Opt. Express* **11**, 1328 (2003), <http://www.opticsexpress.org>.